SUPPLEMENTARY MATERIAL for:

From proteins to polysaccharides; lifestyle and genetic evolution of *Coprothermobacter proteolyticus*.

B.J. Kunath, F. Delogu, A.E. Naas, M.Ø. Arntzen, V.G.H. Eijsink, B. Henrissat, T.R. Hvidsten, P.B. Pope

This PDF file includes:

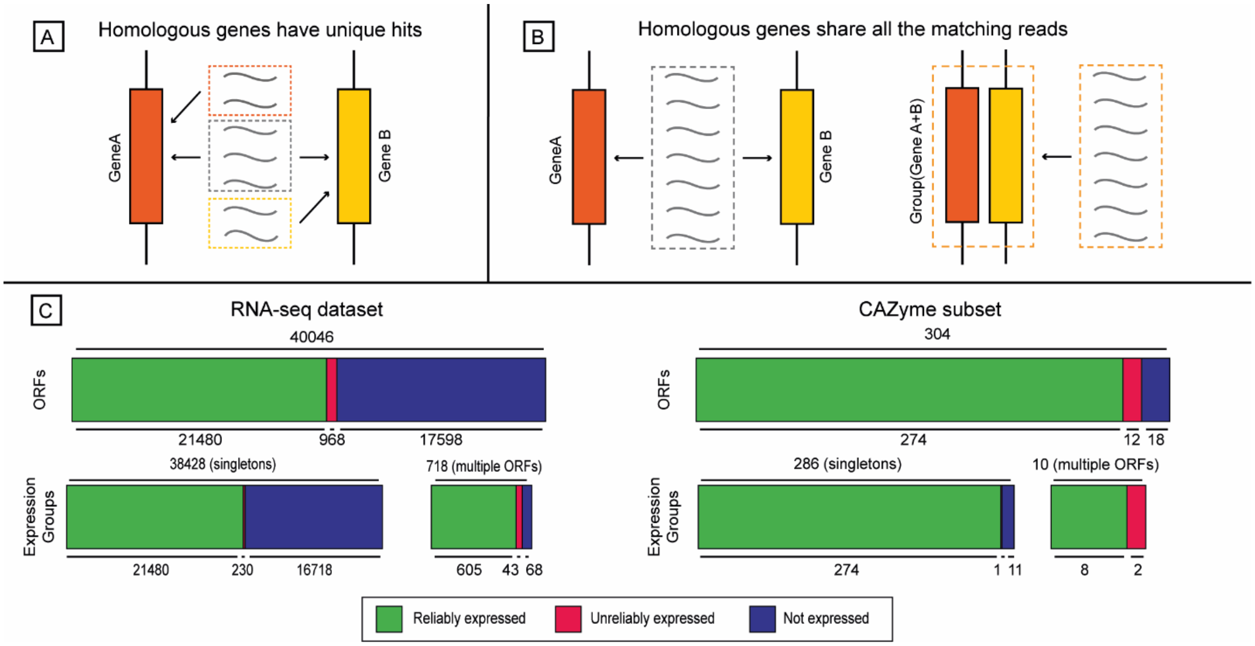

Supplementary Figure 1. Workflow used for RNA-seq quantification and generation of expression groups. **A** and **B** illustrate (respectively) the grouping of genes when unique reads are present (**A**) and when there are not (**B**). In **A,** genes A and B are homologous, and a set of reads maps uniquely to either gene A or to gene B. The subsequent unique sets can be used to sort the ambiguous reads that map on both genes. In **B**, genes A and B are homologous and no unique reads map exclusively to either gene. The two genes cannot be separated and thus their expression cannot be reliably estimated. Instead of losing the information, the genes are merged into an expression group. **C** and **D** represent the effect of collapsing genes into expression groups on the total dataset (**C**), and the reduced dataset focused on CAZymes (**D**).

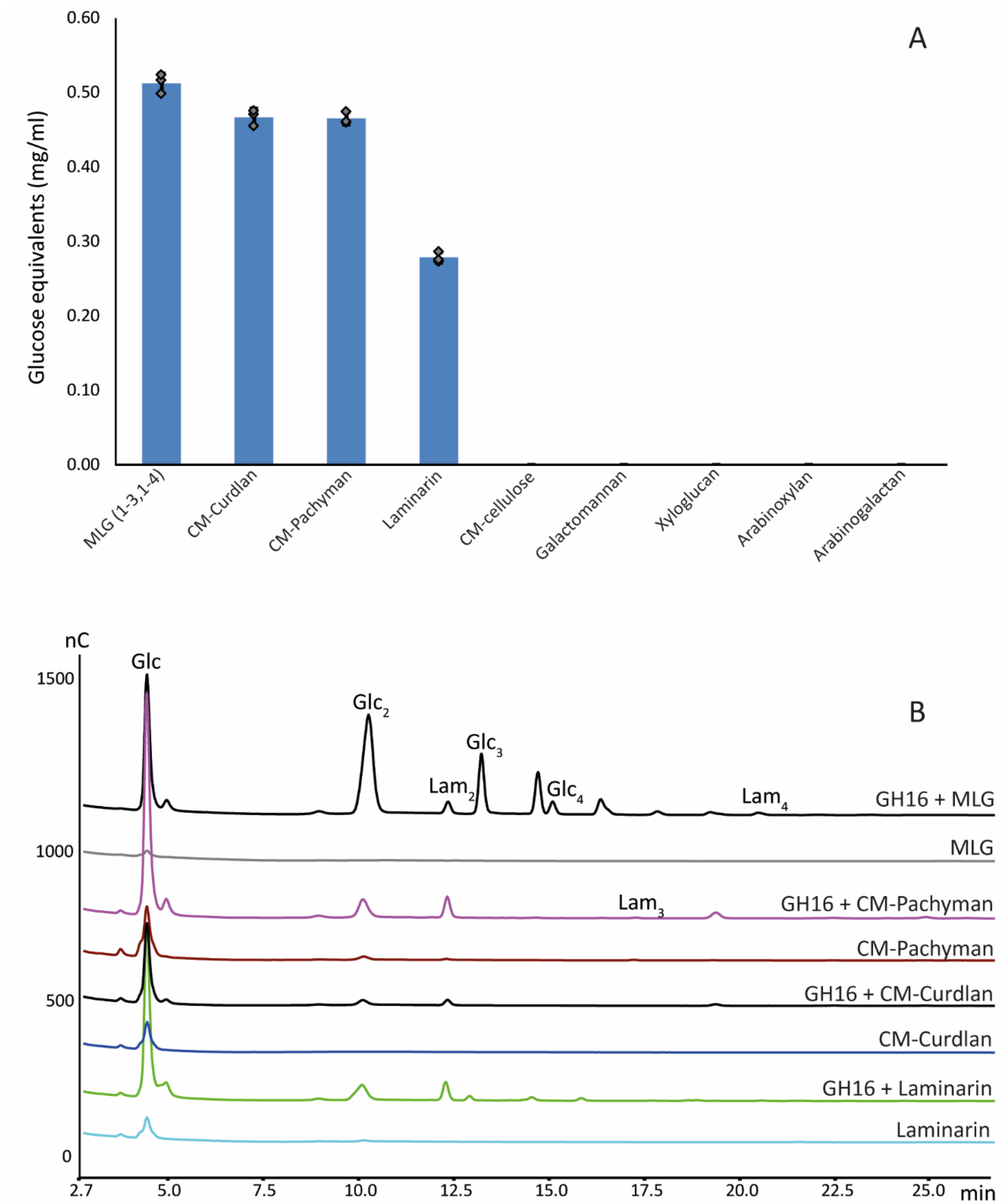

Supplementary Figure 2. Characterization of endo-β-1,3-1,4-glucanase activity by a GH16 CAZyme encoded in BWF2A and SW3C.

A. Degradation of soluble polysaccharides by the GH16 enzyme, measured as reducing ends (glucose equivalents) recovered. Assays were performed at 50°C with 1mg/ml substrate and 1μM enzyme for one hour. Reducing ends were quantified by the DNS-method against a standard curve of glucose. Error bars represent standard deviations among three replicates. The four substrates that yielded activity contain β-1,3 (pachyman, curdlan, laminarin) or mixed β-1,3-1,4-linked glucans (MLG). No activity was exhibited on cellulose (β-1,4 linked glucose), xyloglucans (β-1,4 linked glucose), galactomannan (β-1,4 linked mannose), arabinoxylans (β-1,4 linked xylose) or arabinogalactans (β-1,4 linked galactose). **B.** Degradation products from soluble polysaccharides containing β-1,3-glucan linkages by the GH16 enzyme, analyzed by High-pH anion-exchange chromatography–pulsed amperometric detection (HPAEC-PAD). Identified peaks are annotated as Glc (glucose and cello-oligos) or Lam (laminari-oligos), with their degree of polymerization depicted in subscript. X-axis: retention time in minutes; Y-axis: signal strength (nano-coulombs). For clarity, the chromatograms are shown without the buffer peaks in t=0 - 2.7 min, and from t=27 – 50 min where no peaks were observed. Assays were performed as described above, but reactions were stopped by the addition of NaOH to a final concentration of 0.1M before analysis. CM: Carboxymethyl.

Supplementary Table 1. Anaerobic biogas reactors with reported *Coprothermobacter proteolyticus*-affiliated populations. Date, location, reactor substrate and the presence /absence of cellulose are listed. The SEM1b consortium from this study is highlighted in yellow.

Date	Location	Substrate	Cellulose	Hemicellulose	16S	Reference
2018	Norway I	Cellulose (C)	YES (88.3%)	YES (9.3 %)	YES	This study
2017	Denmark	Food waste, Grass clippings (FW, C)	YES	YES	YES	(Fitamo *et al.*, 2017)
2017	Singapore	wastewater treatment plant sludge (S)	YES	n.a.	YES	(Chen *et al.*, 2017)
2017	Japan I	Acetate/sludge (Ac/S)	NO	NO	YES	(Kouzuma *et al.*, 2017)
2016	Norway II	Food waste (FW)	YES	YES	YES	(Hagen *et al.*, 2017)
2016	S. Korea	Seaweeds (SW)	YES	NO	YES	(Azizi *et al.*, 2016)
2016	Australia I	wastewater treatment plant sludge (S)	n.a.	n.a.	YES	(Ho *et al.*, 2016)
2016	China I	Food waste (FW)	Yes	n.a.	YES	(Chen *et al.*, 2016)
2015	Michigan	wastewater treatment plant sludge (S)	n.a.	n.a.	YES	(Sun *et al.*, 2015)
2015	China II	wastewater treatment plant sludge (S)	n.a.	n.a.	YES	(Yu *et al.*, 2015)
2015	Roma Italy	wastewater treatment plant sludge (S)	NO	NO	YES	(Gagliano *et al.*, 2015)
2014	France	Municipal Solid Waste / Office Paper (C)	YES (70%)	YES (30%)	YES	(Lü *et al.*, 2014)
2013	Australia II	wastewater treatment plant sludge (S)	n.a.	n.a.	YES	(Pervin *et al.*, 2013)
2008	Japan II	wastewater treatment plant sludge (S)	NO	NO	YES	(Kobayashi *et al.*, 2008)

Supplementary Table 2. 16S rRNA analysis of the SEM1b consortium. Taxonomic composition of two separate samples (D1B and D2B), collected from a continuous SEM1b culture. D2B is 15 generations older than D1B. Consensus lineage was determined via QIIME. Closest relatives were determined using BLASTn.

OTU ID	D1B (%)	D2B (%)	Average (%)	Consensus Lineage	Closest relative (BlastN)
OTU-1.1	55.3 (+/- 2.4)	45.2 (+/- 0.2)	50.2	*Clostridium*	*C. thermocellum*
OTU-2.1	26.5 (+/- 1.3)	31.4 (+/- 0.1)	29	*Coprothermobacter*	*C. proteolyticus*
OTU-2.2	10.6 (+/- 0.3)	12.6 (+/- 0.1)	11.6	*Coprothermobacter*	*C. proteolyticus*
OTU-3.1	0	6.9 (+/- 0.04)	3.5	*Anaerobaculum*	*Acetomicrobium mobile*
OTU-4	1.5 (+/- 0.2)	2.8 (+/- 0.1)	2.2	*Tepidimicrobium*	*Tepidimicrobium*
OTU-5	3.7 (+/- 1)	0	1.9	*Clostridium*	*Uncultured bacterium*
OTU-2.3	0.4 (+/- 0.1)	0.4 (+/- 0.03)	0.4	*Coprothermobacter*	*C. proteolyticus*
OTU-3.2	0	0.6 (+/- 0)	0.3	*Anaerobaculum*	*Uncultured Anaerobaculum*
OTU-6.1	1.2 (+/- 0.2)	0	0.6	*Thermoanaerobacterales*	*Tepidanaerobacter*
OTU-6.2	0.7 (+/- 0.2)	0	0.35	*Thermoanaerobacterales*	*Tepidanaerobacter*
OTU-1.2	0.1 (+/- 0)	0	0.05	*Clostridium*	*C. thermocellum*
OTU-7	0.02 (+/- 0.006)	0.02 (+/- 0.005)	0.02	*Methanothermobacter*	*Methanothermobacter*

Supplementary Table 3. CheckM and ANI analyses. Statistics of the metagenome-recovered genomes (MAGs) from the SEM1b consortium as assessed by CheckM and average nucleotide identities (ANI), which were calculated against their closest relative.

MAG Id	Completeness	Contamination	Heterogeneity	Size (Mb)	Closest relative	ANI (%)
RCLO1	98.7	0.0	0.0	3.2	*C. thermocellum* ATCC27405	99.8
COPR1	98.2	5.4	100.0	1.8	*C proteolyticus* DSM5265	97.8
COPR2	0.0	0.0	0.0	0.3	n.a.	n.a.
COPR3	0.0	0.0	0.0	0.3	n.a.	n.a.
SYNG1	86.4	0.0	0.0	1.4	*Acetomicrobium mobile* DSM13181	98.6
SYNG2	13.6	5.1	100.0	0.8	n.a.	n.a.
TISS1	97.9	0.0	0.0	2.1	*Tepidimicrobium xylanilyticum* DSM23310	75.1
TEPI1	82.2	1.7	0.0	1.9	*Tepidanaerobacter acetatoxydans* Re1	74.4
TEPI2	87.0	11.8	14.3	2.4	*Tepidanaerobacter acetatoxydans* Re1	74.6
CLOS1	98.6	1.4	0.0	3.0	*Clostridium Stercorarium* DSM8532	79.1
METH1	99.9	0.0	0.0	1.7	*Methanothermobacter thermautrophicus*	98.2
Unbinned				7.7	n.a.	n.a.

Supplementary Table 4. CAZyme profiles for selected MAGs and genomes. The total number of annotated domains per CAZy family for each SEM1b MAG/genome are listed. * CAZyme profile for *C. proteolyticus* DSM 5265

Supplementary Table 5. Clusters of expression groups. The table shows the gene IMG ID and the CAZy family assignment of each expression group together with the genome and cluster. Groups composed of several ORFs contain a "+" between the gene IDs and the names of the organisms.

Expression Groups (Gene IMG ID)	**CAZy**	**Genome**	**Cluster**
Cluster I: 121 expression groups, 143 domains			
Ga0196617_10021811	CE8	RCLO1	I
Ga0196617_10021811	DOC1	RCLO1	I
Ga0196617_1000051	GH51	CLOS1	I
Ga0196617_10000511	GH138	CLOS1	I
Ga0196617_10000512	GH29	CLOS1	I
Ga0196617_100005134	CE4	CLOS1	I
Ga0196617_10000516	GH2	CLOS1	I
Ga0196617_10000517	CE15	CLOS1	I
Ga0196617_100005175	GH31	CLOS1	I
Ga0196617_10000518	GH95	CLOS1	I
Ga0196617_100005181	CBM25	CLOS1	I
Ga0196617_100005192	GH51	CLOS1	I
Ga0196617_100005195	SLH	CLOS1	I
Ga0196617_100005195	SLH	CLOS1	I
Ga0196617_100005195	SLH	CLOS1	I
Ga0196617_10000520	GH42	CLOS1	I
Ga0196617_100005203	GH2	CLOS1	I
Ga0196617_10000534	GH35	CLOS1	I
Ga0196617_1000055	GH36	CLOS1	I
Ga0196617_1000056	GH36	CLOS1	I
Ga0196617_10000567	GH13_31	CLOS1	I
Ga0196617_10000568	GH36	CLOS1	I
Ga0196617_1000057	GH105	CLOS1	I
Ga0196617_10000579	GH10	CLOS1	I
Ga0196617_1000058	GH3	CLOS1	I
Ga0196617_10000586	GH43	CLOS1	I
Ga0196617_1000059	GH31	CLOS1	I
Ga0196617_100006118	GH43	CLOS1	I
Ga0196617_100006212	CE8	CLOS1	I
Ga0196617_10000638	GH18	CLOS1	I
Ga0196617_10000669	GH88	CLOS1	I
Ga0196617_100011180	GH3	CLOS1	I
Ga0196617_10001122	GH36	CLOS1	I
Ga0196617_10001539	GH67	CLOS1	I
Ga0196617_10001577	CE4	CLOS1	I
Ga0196617_10001596	CE15	CLOS1	I
Ga0196617_10001596	SLH	CLOS1	I
Ga0196617_10001596	SLH	CLOS1	I

Ga0196617_10001596	SLH	CLOS1	I
Ga0196617_100018109	GH133	CLOS1	I
Ga0196617_100018129	GH2	CLOS1	I
Ga0196617_100018135	CE4	CLOS1	I
Ga0196617_10001814	CBM50	CLOS1	I
Ga0196617_10001876	CE7	CLOS1	I
Ga0196617_100020114	GH112	CLOS1	I
Ga0196617_100020115	GH127	CLOS1	I
Ga0196617_100020127	GH63	CLOS1	I
Ga0196617_10002033	CBM48	CLOS1	I
Ga0196617_10002033	GH13_9	CLOS1	I
Ga0196617_10002040	GH29	CLOS1	I
Ga0196617_10002041	GH95	CLOS1	I
Ga0196617_10002065	GH43	CLOS1	I
Ga0196617_10002712	GH2	CLOS1	I
Ga0196617_1000274	GH23	CLOS1	I
Ga0196617_10002766	GH38	CLOS1	I
Ga0196617_10002771	GH105	CLOS1	I
Ga0196617_10002776	GH105	CLOS1	I
Ga0196617_10002777	CE12	CLOS1	I
Ga0196617_10002778	GH105	CLOS1	I
Ga0196617_10002780	GH140	CLOS1	I
Ga0196617_10002785	GH78	CLOS1	I
Ga0196617_1000344	CE9	CLOS1	I
Ga0196617_10003461	GH2	CLOS1	I
Ga0196617_10003498	GH38	CLOS1	I
Ga0196617_10003636	GH43	CLOS1	I
Ga0196617_10003637	GH43	CLOS1	I
Ga0196617_10003684	CBM50	CLOS1	I
Ga0196617_10003684	CBM50	CLOS1	I
Ga0196617_10003849	GH15	CLOS1	I
Ga0196617_10003852	GH95	CLOS1	I
Ga0196617_10003870	GH3	CLOS1	I
Ga0196617_10003880	GH2	CLOS1	I
Ga0196617_10005912	GH28	CLOS1	I
Ga0196617_10005913	GH105	CLOS1	I
Ga0196617_10005914	GH43	CLOS1	I
Ga0196617_10005958	GH39	CLOS1	I
Ga0196617_10005959	GH95	CLOS1	I
Ga0196617_10006041	GH130	CLOS1	I
Ga0196617_1000651	CBM50	CLOS1	I
Ga0196617_10006557	GH73	CLOS1	I
Ga0196617_10006557	SLH	CLOS1	I
Ga0196617_10007036	CBM50	CLOS1	I

Ga0196617_10007036	CBM50	CLOS1	I
Ga0196617_10007036	GH18	CLOS1	I
Ga0196617_10007049	GH94	CLOS1	I
Ga0196617_1000758	GH1	CLOS1	I
Ga0196617_10007748	GH4	CLOS1	I
Ga0196617_10007750	CBM66	CLOS1	I
Ga0196617_10009212	GH13_18	CLOS1	I
Ga0196617_10009249	GH2	CLOS1	I
Ga0196617_1001112	GH42	CLOS1	I
Ga0196617_10011120	GH3	CLOS1	I
Ga0196617_10011122	GH130	CLOS1	I
Ga0196617_10011128	GH88	CLOS1	I
Ga0196617_10011129	GH88	CLOS1	I
Ga0196617_10011135	GH78	CLOS1	I
Ga0196617_10011136	GH3	CLOS1	I
Ga0196617_10011620	GH43	CLOS1	I
Ga0196617_10011624	GH105	CLOS1	I
Ga0196617_1001205	GH4	CLOS1	I
Ga0196617_10015018	GH51	CLOS1	I
Ga0196617_1001561	DOC1	CLOS1	I
Ga0196617_10015626	GH4	CLOS1	I
Ga0196617_1001563	GH4	CLOS1	I
Ga0196617_1001793	GH120	CLOS1	I
Ga0196617_10019216	CBM50	CLOS1	I
Ga0196617_10019216	CBM50	CLOS1	I
Ga0196617_10019218	GH18	CLOS1	I
Ga0196617_10019320	CBM6	CLOS1	I
Ga0196617_1002039	SLH	CLOS1	I
Ga0196617_1002039	SLH	CLOS1	I
Ga0196617_1002039	SLH	CLOS1	I
Ga0196617_1002039	CBM54	CLOS1	I
Ga0196617_10022114	SLH	CLOS1	I
Ga0196617_10022114	SLH	CLOS1	I
Ga0196617_10022114	SLH	CLOS1	I
Ga0196617_10022114	GH18	CLOS1	I
Ga0196617_1002911	GH23	CLOS1	I
Ga0196617_10029410	GH10	CLOS1	I
Ga0196617_1004705	GH35	CLOS1	I
Ga0187557_1002153	CE9	BWF2A	I
Ga0187564_10677	GH18	SW3C	I
Ga0196617_10006619	GH23	COPR1	I
Ga0196617_1005697	GH73	COPR1	I
Ga0196617_1009463	CE9	COPR1	I
Ga0196617_100004229	CBM50	TISS1	I

Ga0196617_100007288	GH3	TISS1	I
Ga0196617_100007296	CE4	TISS1	I
Ga0196617_100010202	GH144	TISS1	I
Ga0196617_100010202	GH94	TISS1	I
Ga0196617_10001251	CBM50	TISS1	I
Ga0196617_10001251	CBM50	TISS1	I
Ga0196617_10001251	CBM50	TISS1	I
Ga0196617_10001251	CBM50	TISS1	I
Ga0196617_10002881	CE4	TISS1	I
Ga0196617_10003113	GH18	TISS1	I
Ga0196617_10004218	CBM50	TISS1	I
Ga0196617_10004240	CE4	TISS1	I
Ga0196617_10005467	GH23	TISS1	I
Ga0187557_1002248 + Ga0187564_10674	GH16	BWF2A + SW3C	I
Ga0187557_100434 + Ga0187564_10433	GH23	BWF2A + SW3C	I
Ga0187557_1002249 + Ga0187564_10675	GH3	BWF2A + SW3C	I
Ga0196617_10009442 + Ga0187564_10367	CBM66	SW3C + COPR1	I
Cluster II: 10 expression groups			
Ga0187557_100243	GH57	BWF2A	II
Ga0187557_1002195	CE4	BWF2A	II
Ga0187557_100472	GH13_m45	BWF2A	II
Ga0187557_1004109	GH23	BWF2A	II
Ga0196617_10006233	GH57	COPR1	II
Ga0196617_10006234	GH57	COPR1	II
Ga0196617_10006658	GH13_m45	COPR1	II
Ga0196617_1001466	GH23	COPR1	II
Ga0196617_10031312	CE4	COPR1	II
Ga0187557_100244 + Ga0187564_103146	GH57	BWF2A + SW3C	II
Cluster III: 10 expression groups, 13 domains			
Ga0196617_10001656	DOC1	RCLO1	III
Ga0196617_10002366	GH1	RCLO1	III
Ga0196617_10003575	DOC1	RCLO1	III
Ga0196617_1000454	CE1	RCLO1	III
Ga0196617_1000454	CBM6	RCLO1	III
Ga0196617_1000454	DOC1	RCLO1	III
Ga0196617_10009713	CBM50	RCLO1	III
Ga0196617_10012635	CBM50	RCLO1	III
Ga0196617_10012635	CBM50	RCLO1	III
Ga0187564_10322	CE9	SW3C	III
Ga0187564_103147	GH57	SW3C	III
Ga0187564_104108	GH23	SW3C	III
Ga0196617_1002669	GH4	COPR3	III
Cluster IV: 11 expression groups, 13 domains			
Ga0196617_10001933	CBM25	RCLO1	IV

Ga0196617_10003643	CE9	CLOS1	IV
Ga0187557_1003280	GH73	BWF2A	IV
Ga0187564_10471	GH13_m45	SW3C	IV
Ga0196617_1000499	GH23	COPR1	IV
Ga0196617_1000628	CE9	COPR1	IV
Ga0196617_1006112	CE4	COPR1	IV
Ga0196617_10001250	CBM50	TISS1	IV
Ga0196617_10001250	CBM50	TISS1	IV
Ga0196617_10001250	CBM50	TISS1	IV
Ga0187564_101146 + Ga0187557_1001161	GH23	BWF2A + SW3C	IV
Ga0187557_1002314 + Ga0187564_106139	GH13_39	BWF2A + SW3C	IV
Ga0187557_100270 + Ga0187564_103120	CE9	BWF2A + SW3C	IV
Cluster V: 28 expression groups, 58 domains			
Ga0196617_10001610	CBM3	RCLO1	V
Ga0196617_10001610	SLH	RCLO1	V
Ga0196617_10001610	SLH	RCLO1	V
Ga0196617_10001610	SLH	RCLO1	V
Ga0196617_10002319	GH5	RCLO1	V
Ga0196617_10003979	CBM50	RCLO1	V
Ga0196617_10004156	DOC1	RCLO1	V
Ga0196617_10004178	GH130	RCLO1	V
Ga0196617_10004620	GH3	RCLO1	V
Ga0196617_10004621	CBM3	RCLO1	V
Ga0196617_10004621	CBM4	RCLO1	V
Ga0196617_10004635	GH43	RCLO1	V
Ga0196617_10004635	CBM6	RCLO1	V
Ga0196617_10004635	CBM6	RCLO1	V
Ga0196617_10004635	DOC1	RCLO1	V
Ga0196617_10004637	CBM42	RCLO1	V
Ga0196617_10006310	GH5_37	RCLO1	V
Ga0196617_10006312	CBM16	RCLO1	V
Ga0196617_10006312	CBM16	RCLO1	V
Ga0196617_1000638	SLH	RCLO1	V
Ga0196617_1000638	SLH	RCLO1	V
Ga0196617_1000638	SLH	RCLO1	V
Ga0196617_1000638	CBM54	RCLO1	V
Ga0196617_1000638	GH16	RCLO1	V
Ga0196617_1000638	CBM4	RCLO1	V
Ga0196617_1000638	CBM4	RCLO1	V
Ga0196617_1000638	CBM4	RCLO1	V
Ga0196617_1000638	CBM4	RCLO1	V
Ga0196617_10007916	CE1	RCLO1	V
Ga0196617_10007916	CBM6	RCLO1	V
Ga0196617_10007916	DOC1	RCLO1	V

Ga0196617_10007916	GH10	RCLO1	V
Ga0196617_1000831	DOC1	RCLO1	V
Ga0196617_10012135	GH9	RCLO1	V
Ga0196617_10012135	CBM3	RCLO1	V
Ga0196617_10012135	DOC1	RCLO1	V
Ga0196617_10012136	DOC1	RCLO1	V
Ga0196617_10012833	CBM3	RCLO1	V
Ga0196617_10013919	GH16	RCLO1	V
Ga0196617_10013919	DOC1	RCLO1	V
Ga0196617_10015134	DOC1	RCLO1	V
Ga0196617_10024516	CE4	RCLO1	V
Ga0196617_10024517	GH11	RCLO1	V
Ga0196617_10024517	CBM6	RCLO1	V
Ga0196617_10024517	DOC1	RCLO1	V
Ga0196617_10024518	GH11	RCLO1	V
Ga0196617_10024518	CBM6	RCLO1	V
Ga0196617_10024518	DOC1	RCLO1	V
Ga0196617_1006901	GH11	RCLO1	V
Ga0196617_100005248	CBM22	CLOS1	V
Ga0196617_100005248	CBM22	CLOS1	V
Ga0196617_100005248	GH10	CLOS1	V
Ga0196617_100005248	CBM9	CLOS1	V
Ga0196617_10000543	GH130	CLOS1	V
Ga0196617_100006227	GH10	CLOS1	V
Ga0196617_100006228	GH30	CLOS1	V
Ga0196617_100006228	CBM22	CLOS1	V
Ga0196617_10001149	GH31	CLOS1	V
Cluster VI: 101 expression groups, 208 domains			
Ga0196617_100009115	GH43	RCLO1	VI
Ga0196617_100009115	CBM13	RCLO1	VI
Ga0196617_100009115	DOC1	RCLO1	VI
Ga0196617_100009116	GH81	RCLO1	VI
Ga0196617_100009116	DOC1	RCLO1	VI
Ga0196617_100009142	DOC1	RCLO1	VI
Ga0196617_100009143	CBM48	RCLO1	VI
Ga0196617_100009158	GH9	RCLO1	VI
Ga0196617_100009158	CBM3	RCLO1	VI
Ga0196617_100009158	DOC1	RCLO1	VI
Ga0196617_100009159	CBM30	RCLO1	VI
Ga0196617_100009159	GH9	RCLO1	VI
Ga0196617_100009159	GH44	RCLO1	VI
Ga0196617_100009159	DOC1	RCLO1	VI
Ga0196617_100009159	CBM44	RCLO1	VI
Ga0196617_100009203	GH9	RCLO1	VI

Ga0196617_100009203	CBM3	RCLO1	VI
Ga0196617_100009203	DOC1	RCLO1	VI
Ga0196617_100009224	CE4	RCLO1	VI
Ga0196617_10000923	GH9	RCLO1	VI
Ga0196617_10000923	CBM3	RCLO1	VI
Ga0196617_10000923	DOC1	RCLO1	VI
Ga0196617_10000943	DOC1	RCLO1	VI
Ga0196617_100014143	GH9	RCLO1	VI
Ga0196617_100014143	DOC1	RCLO1	VI
Ga0196617_100014145	GH5_55	RCLO1	VI
Ga0196617_100014145	CBM32	RCLO1	VI
Ga0196617_100014145	DOC1	RCLO1	VI
Ga0196617_10001446	DOC1	RCLO1	VI
Ga0196617_10001451	CBM22	RCLO1	VI
Ga0196617_10001451	GH10	RCLO1	VI
Ga0196617_10001451	CBM22	RCLO1	VI
Ga0196617_10001451	DOC1	RCLO1	VI
Ga0196617_10001451	CE1	RCLO1	VI
Ga0196617_1000146	CBM25	RCLO1	VI
Ga0196617_10001484	GH23	RCLO1	VI
Ga0196617_100016107	SLH	RCLO1	VI
Ga0196617_100016107	SLH	RCLO1	VI
Ga0196617_10001684	CBM22	RCLO1	VI
Ga0196617_10001684	GH10	RCLO1	VI
Ga0196617_10001684	DOC1	RCLO1	VI
Ga0196617_10001939	CE4	RCLO1	VI
Ga0196617_10002318	GH26	RCLO1	VI
Ga0196617_10002318	GH5_25	RCLO1	VI
Ga0196617_10002318	CBM11	RCLO1	VI
Ga0196617_10002318	DOC1	RCLO1	VI
Ga0196617_10002394	GH53	RCLO1	VI
Ga0196617_10002394	DOC1	RCLO1	VI
Ga0196617_10002396	GH74	RCLO1	VI
Ga0196617_10002396	DOC1	RCLO1	VI
Ga0196617_100024103	CBM3	RCLO1	VI
Ga0196617_100024109	SLH	RCLO1	VI
Ga0196617_100024109	SLH	RCLO1	VI
Ga0196617_100024109	SLH	RCLO1	VI
Ga0196617_10002441	GH133	RCLO1	VI
Ga0196617_10002490	GH48	RCLO1	VI
Ga0196617_10002490	CBM3	RCLO1	VI
Ga0196617_10002537	DOC1	RCLO1	VI
Ga0196617_10002537	DOC1	RCLO1	VI
Ga0196617_100026113	DOC1	RCLO1	VI

Ga0196617_10002620	GH10	RCLO1	VI
Ga0196617_10002651	GH48	RCLO1	VI
Ga0196617_10002651	DOC1	RCLO1	VI
Ga0196617_10003325	DOC1	RCLO1	VI
Ga0196617_10003331	CBM50	RCLO1	VI
Ga0196617_10003331	CBM50	RCLO1	VI
Ga0196617_10003331	GH18	RCLO1	VI
Ga0196617_10003345	GH15	RCLO1	VI
Ga0196617_100035100	CBM4	RCLO1	VI
Ga0196617_100035100	GH9	RCLO1	VI
Ga0196617_100035100	CBM3	RCLO1	VI
Ga0196617_100035100	DOC1	RCLO1	VI
Ga0196617_100035101	GH9	RCLO1	VI
Ga0196617_100035101	DOC1	RCLO1	VI
Ga0196617_10003578	DOC1	RCLO1	VI
Ga0196617_10003578	GH124	RCLO1	VI
Ga0196617_10003580	GH9	RCLO1	VI
Ga0196617_10003580	CBM3	RCLO1	VI
Ga0196617_10003580	DOC1	RCLO1	VI
Ga0196617_10003956	GH3	RCLO1	VI
Ga0196617_10004017	GH94	RCLO1	VI
Ga0196617_10004018	GH9	RCLO1	VI
Ga0196617_10004018	DOC1	RCLO1	VI
Ga0196617_10004021	CBM3	RCLO1	VI
Ga0196617_10004022	GH18	RCLO1	VI
Ga0196617_10004022	DOC1	RCLO1	VI
Ga0196617_10004023	GH8	RCLO1	VI
Ga0196617_10004023	DOC1	RCLO1	VI
Ga0196617_10004025	CBM3	RCLO1	VI
Ga0196617_10004034	DOC1	RCLO1	VI
Ga0196617_10004046	DOC1	RCLO1	VI
Ga0196617_10004046	CBM35	RCLO1	VI
Ga0196617_10004053	DOC1	RCLO1	VI
Ga0196617_10004125	CBM25	RCLO1	VI
Ga0196617_10004148	CBM35	RCLO1	VI
Ga0196617_10004148	CE12	RCLO1	VI
Ga0196617_10004149	CE12	RCLO1	VI
Ga0196617_10004149	DOC1	RCLO1	VI
Ga0196617_1000447	SLH	RCLO1	VI
Ga0196617_1000447	SLH	RCLO1	VI
Ga0196617_1000447	SLH	RCLO1	VI
Ga0196617_10004476	SLH	RCLO1	VI
Ga0196617_10004476	SLH	RCLO1	VI
Ga0196617_10004476	SLH	RCLO1	VI

Ga0196617_1000451	CBM6	RCLO1	VI
Ga0196617_1000451	DOC1	RCLO1	VI
Ga0196617_1000452	GH43	RCLO1	VI
Ga0196617_1000452	CBM6	RCLO1	VI
Ga0196617_1000452	DOC1	RCLO1	VI
Ga0196617_10004521	DOC1	RCLO1	VI
Ga0196617_10004521	CBM35	RCLO1	VI
Ga0196617_1000453	GH141	RCLO1	VI
Ga0196617_1000453	CBM6	RCLO1	VI
Ga0196617_1000453	DOC1	RCLO1	VI
Ga0196617_10004533	GH126	RCLO1	VI
Ga0196617_10004546	SLH	RCLO1	VI
Ga0196617_10004546	SLH	RCLO1	VI
Ga0196617_10004546	SLH	RCLO1	VI
Ga0196617_1000455	GH43	RCLO1	VI
Ga0196617_1000455	CBM6	RCLO1	VI
Ga0196617_1000455	DOC1	RCLO1	VI
Ga0196617_10004553	CBM3	RCLO1	VI
Ga0196617_10004553	GH5_1	RCLO1	VI
Ga0196617_10004553	DOC1	RCLO1	VI
Ga0196617_1000458	CBM48	RCLO1	VI
Ga0196617_1000458	GH13_9	RCLO1	VI
Ga0196617_1000459	CE9	RCLO1	VI
Ga0196617_1000635	GH9	RCLO1	VI
Ga0196617_1000635	DOC1	RCLO1	VI
Ga0196617_10006355	GH9	RCLO1	VI
Ga0196617_10006355	CBM3	RCLO1	VI
Ga0196617_10006355	DOC1	RCLO1	VI
Ga0196617_10006356	GH9	RCLO1	VI
Ga0196617_10006356	CBM3	RCLO1	VI
Ga0196617_10006356	CBM3	RCLO1	VI
Ga0196617_10006356	DOC1	RCLO1	VI
Ga0196617_1000636	CBM35	RCLO1	VI
Ga0196617_1000636	GH26	RCLO1	VI
Ga0196617_1000636	DOC1	RCLO1	VI
Ga0196617_1000731	SLH	RCLO1	VI
Ga0196617_1000731	SLH	RCLO1	VI
Ga0196617_1000731	SLH	RCLO1	VI
Ga0196617_10007316	GH94	RCLO1	VI
Ga0196617_10008321	CBM6	RCLO1	VI
Ga0196617_1000954	CBM22	RCLO1	VI
Ga0196617_1000954	GH10	RCLO1	VI
Ga0196617_1000954	DOC1	RCLO1	VI
Ga0196617_1000961	CBM4	RCLO1	VI

Ga0196617_1000961	GH9	RCLO1	VI
Ga0196617_10009628	DOC1	RCLO1	VI
Ga0196617_1000968	GH5_1	RCLO1	VI
Ga0196617_1000968	DOC1	RCLO1	VI
Ga0196617_1000969	CBM3	RCLO1	VI
Ga0196617_10009710	SLH	RCLO1	VI
Ga0196617_10009729	CBM50	RCLO1	VI
Ga0196617_10010817	GH23	RCLO1	VI
Ga0196617_1001211	CBM42	RCLO1	VI
Ga0196617_1001211	DOC1	RCLO1	VI
Ga0196617_1001211	GH43	RCLO1	VI
Ga0196617_10012123	CBM35	RCLO1	VI
Ga0196617_10012123	GH26	RCLO1	VI
Ga0196617_10012123	DOC1	RCLO1	VI
Ga0196617_10012132	GH9	RCLO1	VI
Ga0196617_10012132	CBM3	RCLO1	VI
Ga0196617_10012132	CBM3	RCLO1	VI
Ga0196617_10012516	GH9	RCLO1	VI
Ga0196617_10012516	CBM3	RCLO1	VI
Ga0196617_10012516	DOC1	RCLO1	VI
Ga0196617_1001259	GH5_1	RCLO1	VI
Ga0196617_1001259	DOC1	RCLO1	VI
Ga0196617_10012616	GH94	RCLO1	VI
Ga0196617_10012633	CBM50	RCLO1	VI
Ga0196617_10012633	CBM50	RCLO1	VI
Ga0196617_10012633	CBM50	RCLO1	VI
Ga0196617_10012633	CBM50	RCLO1	VI
Ga0196617_10012634	CBM50	RCLO1	VI
Ga0196617_10012634	CBM50	RCLO1	VI
Ga0196617_10012634	CBM50	RCLO1	VI
Ga0196617_10012713	DOC1	RCLO1	VI
Ga0196617_10012729	GH18	RCLO1	VI
Ga0196617_1001275	GH5_1	RCLO1	VI
Ga0196617_1001275	DOC1	RCLO1	VI
Ga0196617_1001361	CE3	RCLO1	VI
Ga0196617_1001361	CE3	RCLO1	VI
Ga0196617_1001361	DOC1	RCLO1	VI
Ga0196617_1001363	GH5_4	RCLO1	VI
Ga0196617_1001363	DOC1	RCLO1	VI
Ga0196617_1001363	CE2	RCLO1	VI
Ga0196617_1001365	CBM34	RCLO1	VI
Ga0196617_1001365	GH13_20	RCLO1	VI
Ga0196617_10013921	GH1	RCLO1	VI
Ga0196617_10014123	CE14	RCLO1	VI

Ga0196617_1001491	SLH	RCLO1	VI
Ga0196617_1001491	SLH	RCLO1	VI
Ga0196617_1001492	SLH	RCLO1	VI
Ga0196617_1001492	SLH	RCLO1	VI
Ga0196617_10015133	DOC1	RCLO1	VI
Ga0196617_10019617	GH9	RCLO1	VI
Ga0196617_10019617	CBM3	RCLO1	VI
Ga0196617_10019617	CBM3	RCLO1	VI
Ga0196617_10019617	DOC1	RCLO1	VI
Ga0196617_1002189	DOC1	RCLO1	VI
Ga0196617_1002189	CBM35	RCLO1	VI
Ga0196617_1002401	CBM3	RCLO1	VI
Ga0196617_1005678	CE7	RCLO1	VI
Ga0196617_1008651	GH2	RCLO1	VI
Ga0196617_1008651	CBM6	RCLO1	VI
Ga0196617_100012177	CBM50	TISS1	VI

Supplementary Table 6. Genome IMG ID and SRA numbers for datasets used in this study

Dataset	SRA Accession number	IMG Genome ID
Metagenomes		
SEM1b_D1B	SRX3777359	3300019285
SEM1b_D2B	SRX3777360	3300019285
SEM1b_D1B-r1 (16S rRNA)	SRX3777358	
SEM1b_D2B-r1 (16S rRNA)	SRX3777363	
SEM1b_D1B-r2 (16S rRNA)	SRX3777361	
SEM1b_D2B-r2 (16S rRNA)	SRX3777362	
Isolate genomes		
C. proteolyticus BWF2A	SRX3783215	2731957509
C. proteolyticus SW3C	SRX3783214	2731957514
SEM1b time series		
Dataset	**Metatranscriptomes**	**16S rRNA**
SEM1b_T1A		SRX3777365
SEM1b_T1B		SRX3777364
SEM1b_T1C		SRX3777357
SEM1b_T2A	SRX3777356	SRX3777346
SEM1b_T2B	SRX3777345	SRX3777348
SEM1b_T2C	SRX3777347	SRX3777350
SEM1b_T3A	SRX3777349	SRX3777352
SEM1b_T3B	SRX3777351	SRX3777354
SEM1b_T3C	SRX3777353	SRX3777368
SEM1b_T4A	SRX3777369	SRX3777370
SEM1b_T4B	SRX3777371	SRX3777372
SEM1b_T4C	SRX3777373	SRX3777374
SEM1b_T5A	SRX3777375	SRX3777366
SEM1b_T5B	SRX3777367	SRX3777344
SEM1b_T5C	SRX3777343	SRX3777342
SEM1b_T6A	SRX3777341	SRX3777340
SEM1b_T6B	SRX3777339	SRX3777338
SEM1b_T6C	SRX3777337	SRX3777336
SEM1b_T7A	SRX3777335	SRX3777384
SEM1b_T7B	SRX3777385	SRX3777382
SEM1b_T7C	SRX3777383	SRX3777380
SEM1b_T8A	SRX3777381	SRX3777378
SEM1b_T8B	SRX3777379	SRX3777376
SEM1b_T8C	SRX3777377	SRX3777355

REFERENCES.

Azizi A, Kim W, Lee JH (2016). Comparison of microbial communities during the anaerobic digestion of Gracilaria under mesophilic and thermophilic conditions. *World Journal of Microbiology and Biotechnology* **32:** 1-17.

Chen Y, Zhang F, Wang T, Shen N, Yu ZW, Zeng RJ (2016). Hydraulic retention time affects stable acetate production from tofu processing wastewater in extreme-thermophilic (70 °C) mixed culture fermentation. *Bioresource Technology* **216:** 722-728.

Chen Y, Xiao K, Jiang X, Shen N, Zeng RJ, Zhou Y (2017). In-situ sludge pretreatment in a single-stage anaerobic digester. *Bioresource Technology* **238:** 102-108.

Fitamo T, Treu L, Boldrin A, Sartori C, Angelidaki I, Scheutz C (2017). Microbial population dynamics in urban organic waste anaerobic co-digestion with mixed sludge during a change in feedstock composition and different hydraulic retention times. *Water Research* **118:** 261-271.

Gagliano MC, Braguglia CM, Gianico A, Mininni G, Nakamura K, Rossetti S (2015). Thermophilic anaerobic digestion of thermal pretreated sludge: Role of microbial community structure and correlation with process performances. *Water Research* **68:** 498-509.

Hagen LH, Frank JA, Zamanzadeh M, Eijsink VGH, Pope PB, Horn SJ *et al* (2017). Quantitative metaproteomics highlight the metabolic contributions of uncultured phylotypes in a thermophilic anaerobic digester. *Applied and Environmental Microbiology* **83**.

Ho D, Jensen P, Gutierrez-Zamora ML, Beckmann S, Manefield M, Batstone D (2016). High-rate, high temperature acetotrophic methanogenesis governed by a three population consortium in anaerobic bioreactors. *PLoS ONE* **11:** 1-13.

Kobayashi T, Li YY, Harada H (2008). Analysis of microbial community structure and diversity in the thermophilic anaerobic digestion of waste activated sludge. *Water Science and Technology* **57:** 1199-1205.

Kouzuma A, Tsutsumi M, Ishii Si, Ueno Y, Abe T, Watanabe K (2017). Non-autotrophic methanogens dominate in anaerobic digesters. *Scientific Reports* **7:** 1-13.

Lü F, Bize A, Guillot A, Monnet V, Madigou C, Chapleur O *et al* (2014). Metaproteomics of cellulose methanisation under thermophilic conditions reveals a surprisingly high proteolytic activity. *ISME Journal* **8:** 88-102.

Pervin HM, Dennis PG, Lim HJ, Tyson GW, Batstone DJ, Bond PL (2013). Drivers of microbial community composition in mesophilic and thermophilic temperature-phased anaerobic digestion pre-treatment reactors. *Water Research* **47:** 7098-7108.

Sun W, Yu G, Louie T, Liu T, Zhu C, Xue G *et al* (2015). From mesophilic to thermophilic digestion: the transitions of anaerobic bacterial, archaeal, and fungal community structures in sludge and manure samples. *Applied Microbiology and Biotechnology* **99:** 10271-10282.

Yu B, Lou Z, Zhang D, Shan A, Yuan H, Zhu N *et al* (2015). Variations of organic matters and microbial community in thermophilic anaerobic digestion of waste activated sludge with the addition of ferric salts. *Bioresource Technology* **179:** 291-298.